
Effects of anisotropy on elastic moduli measured by nanoindentation in human tibial cortical bone

J. G. Swadener,^{1,2} Jae-Young Rho,³ G. M. Pharr^{1,2}

¹*Metals and Ceramics Division, Oak Ridge National Laboratory, P.O. Box 2008, MS-6093, Oak Ridge, Tennessee 37831-6093*

²*Department of Materials Science and Engineering, University of Tennessee, Knoxville, Tennessee 37996-2200*

³*Department of Biomedical Engineering, University of Memphis, Memphis, Tennessee 38152-6582*

Received 24 July 2000; revised 24 January 2001; accepted 22 March 2001

Abstract: Many biological materials are known to be anisotropic. In particular, microstructural components of biological materials may grow in a preferred direction, giving rise to anisotropy in the microstructure. Nanoindentation has been shown to be an effective technique for determining the mechanical properties of microstructures as small as a few microns. However, the effects of anisotropy on the properties measured by nanoindentation have not been fully addressed. This study presents a method to account for the effects of anisotropy on elastic properties measured by na-

noindentation. This method is used to correlate elastic properties determined from earlier nanoindentation experiments and from earlier ultrasonic velocity measurements in human tibial cortical bone. Also presented is a procedure to determine anisotropic elastic moduli from indentation measurements in multiple directions. © 2001 John Wiley & Sons, Inc. *J Biomed Mater Res* 57: 108–112, 2001

Key words: anisotropy; cortical bone; elastic modulus; nanoindentation; ultrasonic velocity

INTRODUCTION

The elastic properties of bone microstructural components (e.g., osteons, interstitial lamellae, and individual trabeculae) have been determined by various microtesting methods.^{1–10} However, these different experimental techniques have yielded results that vary by a factor of 3 or more both for cortical bone^{11,12} and for single osteons.^{1–4} These results demonstrate the difficulty of fabricating representative small specimens by removal of the surrounding material. Recently, nanoindentation techniques have been found to be effective in determining the moduli of bone constituents without having to remove the surrounding material.^{13–15} These techniques simplify specimen fabrication, greatly reducing the likelihood of damage to the specimen. Nanoindentation is even more advan-

tageous when the structural components are a few microns or less in size, which occurs with some bone microstructures such as individual lamellae in osteons. In addition, nanoindentation can be conducted in different directions to investigate the anisotropy of the individual microstructural components. However, during indentation stresses develop in all directions, which suggests that the modulus measured by indentation will be a combination of the moduli in all directions, albeit weighted in the direction of indentation.^{16–19}

The present study was able to demonstrate how elastic moduli should be combined. It correlated nanoindentation results¹³ with anisotropic elastic moduli determined from ultrasonic velocity measurements²⁰ for human tibial cortical bone.

MATERIALS AND METHODS

Methods

Nanoindentation was conducted on dehydrated bone, whose results¹³ were analyzed and compared with ultrasonic velocity measurements²⁰ obtained

Correspondence to: J. G. Swadener, Los Alamos National Laboratory, MST-8, MS-G755, Los Alamos, NM 87545; e-mail: swadener@lanl.gov

Contract grant sponsor: Division of Materials Sciences and Engineering, U.S. Department of Energy (for research at the Oak Ridge National Laboratory SHaRE user facility); contract grant number: DE-AC05-00OR22725 with UT-Battelle, LLC

from bone specimens kept moist in a saline solution. Dehydration has been shown to increase the elastic moduli of bone by 15–24%.^{10,21,22} In addition, nanoindentation was conducted on specific microstructures (osteons and interstitial lamellae), while the ultrasonic results applied to macroscopic bone specimens. To compare the nanoindentation results to the ultrasonic results, we adopted a rule of mixtures approach, which included a small void fraction, to estimate the anisotropic elastic moduli of the composite bone from the microstructural nanoindentation results. Finally, the effect of dehydration was adjusted so there would be an appropriate basis for comparing the two experimental results.

The general anisotropic small strain formulation of Hooke's law can be conveniently defined using vector representations for stress ($\underline{\sigma}$) and strain ($\underline{\varepsilon}$) and a matrix representation for the elastic stiffness matrix (\underline{C}) as:

$$\underline{\sigma} = \underline{C}\underline{\varepsilon}, \quad (1)$$

where $\{\sigma_i\} = [\sigma_{11}, \sigma_{22}, \sigma_{33}, \sigma_{23}, \sigma_{31}, \sigma_{12}]^T$, $\{\varepsilon_i\} = [\varepsilon_{11}, \varepsilon_{22}, \varepsilon_{33}, 2\varepsilon_{23}, 2\varepsilon_{31}, 2\varepsilon_{12}]^T$ and T is the matrix transpose operation. For general anisotropy in this representation \underline{C} is a symmetric matrix containing 21 independent elastic constants. For orthotropic materials (such as materials with orthorhombic symmetry), the principal axes form three planes of symmetry, reducing the number of independent elastic constants to 9. Human cortical bone has been shown to be orthotropic.²⁰

Nanoindentation experiments are most commonly conducted with sharp pyramidal indenters, preferably three-sided because they can be ground to the sharpest points.²³ However, no exact analytical expressions exist for indentation with a pyramidal tip. Numerical studies^{24,25} have indicated that to match results for three-sided pyramidal tips, a correction factor of $\beta = 1.034$ should be applied to modulus values predicted by a conical tip. Anisotropic materials showed differences of less than 2% in the value of β because of orientation.²⁶

Conical indentation of isotropic materials is well understood,²⁷ but material anisotropy complicates the analysis of results obtained by nanoindentation. Material anisotropy causes one such complication: the displacement of the indented surface varying in different directions, producing a saddle-shaped edge of contact between the indenter and the indented surface, as shown in Figure 1. The contact area projected in a plane parallel to the surface is elliptical, with the long axis of the ellipse passing through the highest points on the edge of contact and the short axis of the ellipse passing through the lowest points.

Swadener and Pharr have recently developed an analysis of conical indentation of anisotropic materials.¹⁹ The ratio of the elliptical axes of the projected

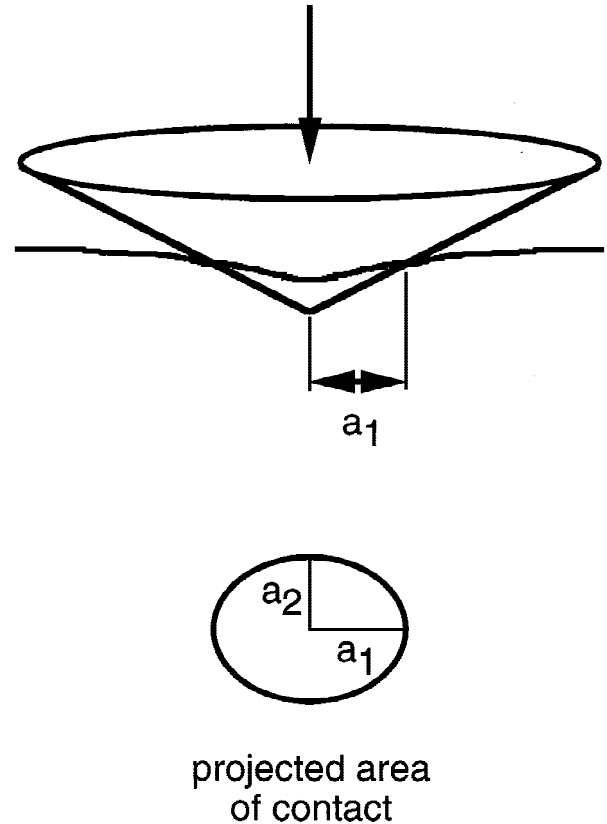


Figure 1. Area of contact during indentation of an anisotropic material.

area of contact (a_1/a_2) for an indentation of an anisotropic surface by a rigid frictionless cone can be found, according to their analysis, by solving numerically the integral equation:

$$\begin{aligned} & \frac{1}{2} \left(1 - \frac{2}{\pi} \sqrt{\frac{a_1}{a_2}} \right) \int_0^{2\pi} \frac{a_{3i} B_{ij}^{-1}(\gamma) a_{3j}}{\sqrt{\left(\frac{a_1}{a_2}\right) \cos^2 \gamma + \left(\frac{a_2}{a_1}\right) \sin^2 \gamma}} d\gamma \\ &= \int_{-\pi/2}^{\pi/2} (1 - |\sin \gamma'|) \frac{a_{3i} B_{ij}^{-1}(\gamma') a_{3j}}{\sqrt{\left(\frac{a_1}{a_2}\right) \cos^2 \gamma' + \left(\frac{a_2}{a_1}\right) \sin^2 \gamma'}} d\gamma'. \end{aligned} \quad (2)$$

where B_{ij} is the components, derived from the elastic stiffness matrix, of the first Barnett–Lothe tensor,²⁸ and a_{3i} and a_{3j} are the direction cosines of the angles between the indentation direction and the directions that define the coefficients of the elastic stiffness matrix. The summation convention is used over repeated indices. If the indented surface possesses mirror symmetry, the contact ellipse is oriented with one axis aligned with the line of symmetry (for other cases, see ref. 19).

In nanoindentation experiments measurements of load and displacement can determine the stiffness of the indentation contact (S). Elastic constants can then

be determined from the contact stiffness. For anisotropic materials Vlassak and Nix¹⁷ showed that an expression for contact stiffness can be used to define an indentation modulus (M):

$$S = \frac{2}{\sqrt{\pi}} M \sqrt{A},$$

where A is the projected area of contact, which can also be determined experimentally.²⁹ For isotropic materials with elastic modulus (E) and Poisson's ratio (ν), Pharr et al.³⁰ showed that $M = E/(1 - \nu^2)$ for any axisymmetric indenter. It is from this relation that the elastic modulus measured by nanoindentation is most frequently evaluated. For indentation of anisotropic materials by cones, paraboloids of revolution, or flat elliptical punches, the indentation modulus can be determined from:¹⁹

$$M = \frac{4\pi}{\int_0^{2\pi} \frac{a_{3i} B_{ij}^{-1}(\gamma) a_{3j}}{\sqrt{\left(\frac{a_1}{a_2}\right) \cos^2 \gamma + \left(\frac{a_2}{a_1}\right) \sin^2 \gamma}} d\gamma}, \quad (4)$$

where, for conical indenters, the ratio a_1/a_2 can be determined from Equation (2). For isotropic materials, Equation (4) reduces to $M = E/(1 - \nu^2)$. However, indentation of general anisotropic materials is distinct, and the indentation modulus varies with direction and depends on the eccentricity of the elliptical projected area of contact.

RESULTS AND DISCUSSION

Nanoindentation experiments are generally conducted with the axis of indentation normal to the surface. In order to assess a material's anisotropy, specimens can be fabricated with various surface orientations. Rho et al.¹³ conducted nanoindentation experiments on human tibial cortical bone in the longitudinal and transverse directions, but at the time of their experiments no means existed for comparing their results to anisotropic elastic constants. To make such a comparison, the indentation modulus (M) was calculated using Equation (4) based on the elastic stiffness components (Table I) determined by Rho²⁰ from ultrasonic velocity measurements. The assumptions $C_{13} = C_{23}$ and $C_{12} = C_{11} - 2C_{66}$ were used for the

remaining two components, which could not be determined from ultrasonic velocity measurements because of the small thickness of tibial cortical bone. Rho²⁰ showed that ultrasonic velocity measurements of human cortical bone correlated well with elastic moduli measured by conventional methods.

The value of M was calculated by numerical integration of Equation (4)—with convergence to within 0.01%—for indentation parallel to the surface normal lying in a principal material plane. The x_1 direction is the radial direction in the tibia, the x_2 direction is the circumferential direction, and the x_3 direction is the superior–inferior direction, as shown in Figure 2. For comparison, the value of the elastic modulus (E) in various directions was calculated using tensor transformations from the data in Table I.³¹ Figure 3 plots the a_1/a_2 ratio for conical indentation parallel to surface normals in the x_1 – x_3 plane and in the x_2 – x_3 plane. For indentation in the x_1 – x_3 plane, the a_1 axis is always parallel to the x_2 direction, and for indentation in the x_2 – x_3 plane, the a_1 axis is parallel to the x_1 direction. As expected, the a_1/a_2 ratio for $\varphi = 90^\circ$, $\theta = 0^\circ$ is the reciprocal of the ratio for $\varphi = 90^\circ$, $\theta = 90^\circ$. The indentation modulus and the elastic modulus for the same range of directions are depicted in Figure 4. As expected, the indentation modulus varies with direction in a manner similar to the elastic modulus. The minimum indentation modulus is greater than the minimum elastic modulus because of the influence of elastic moduli in other directions. The same effect accounts for the variation in the indentation modulus with direction not being as great as the variation in the elastic modulus. The a_1/a_2 ratio and the indentation modulus for conical indentation parallel to surface normals in the x_1 – x_2 plane are plotted in Figure 5, with the a_2 axis always parallel to the x_3 direction. For indentation in the x_1 – x_2 plane, the indentation modulus is always greater than the elastic modulus because of the influence of the larger elastic modulus in the x_3 direction.

The indentation moduli for human tibial cortical bone osteons and interstitial lamellae have been determined from nanoindentation experiments by Rho et al.¹³ for the x_1 and x_3 directions. For indentations in the x_3 direction, they found a mean indentation modulus of 24.6 GPa (standard deviation = 1.3 GPa) for osteons and 28.2 GPa (standard deviation = 1.1 GPa) for interstitial lamellae. For indentations in the x_1 direction, the indentation modulus was 18.2 GPa (standard deviation = 1.2 GPa) for osteons and interstitial

TABLE I
Mean Values of Elastic Stiffness Matrix Components of Human Tibial Cortical Bone (standard deviation in parentheses)

C_{11} (GPa)	C_{22} (GPa)	C_{33} (GPa)	C_{44} (GPa)	C_{55} (GPa)	C_{66} (GPa)	C_{23} (GPa)
19.5 (2.0)	20.1 (1.9)	30.9 (2.1)	5.72 (0.49)	5.17 (0.57)	4.05 (0.54)	12.5 (1.2)

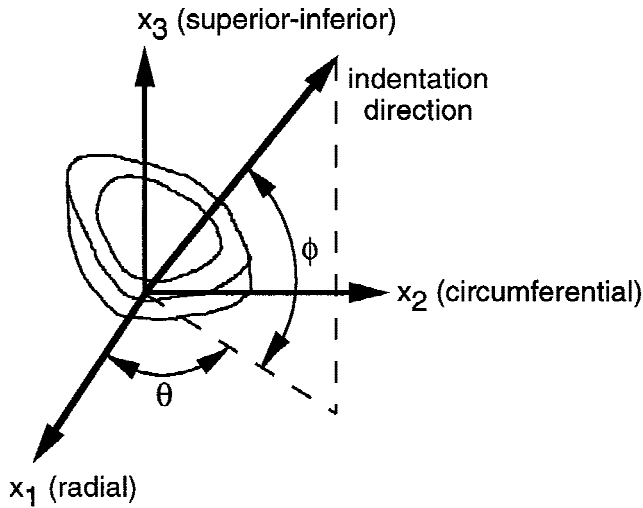


Figure 2. Orientation of the material axes and the angles θ and ϕ , which define the indentation direction.

lamellae combined.¹³ The human tibial cortical bone specimens contained approximately 5% voids, which caused some differences in the moduli, as determined by nanoindentation and ultrasonic velocity measurements. Nanoindentation measures the mechanical response of the solid constituents in the vicinity of the indenter, while ultrasonic velocity measurements are conducted on the composite specimen. A rule of mixtures approach can produce approximate values to enable a comparison. Since the void fraction is small, errors from approximation will be small compared to the uncertainty in the experimental results. Osteons and interstitial lamellae make up approximately equal volumes in cortical bone. Therefore, the nanoindentation data give estimates of combined indentation moduli of 25.1 GPa in the x_3 direction and 17.3 GPa in the x_1 direction. The indentation moduli obtained

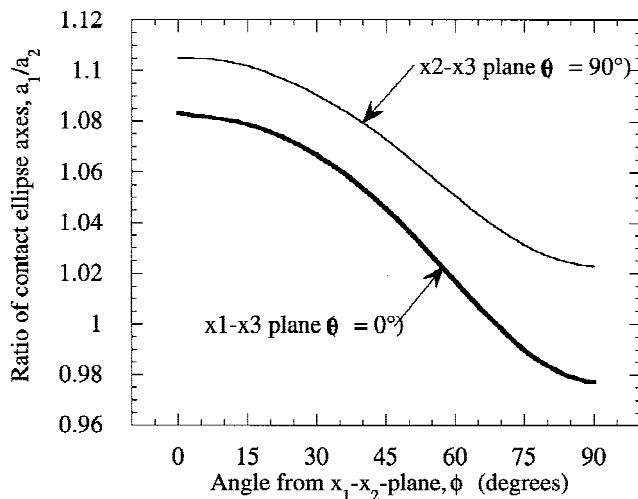


Figure 3. Ratio of elliptical contact axes (a_1/a_2) for conical indentation of human tibial cortical bone in the x_1 - x_3 plane and the x_2 - x_3 plane.

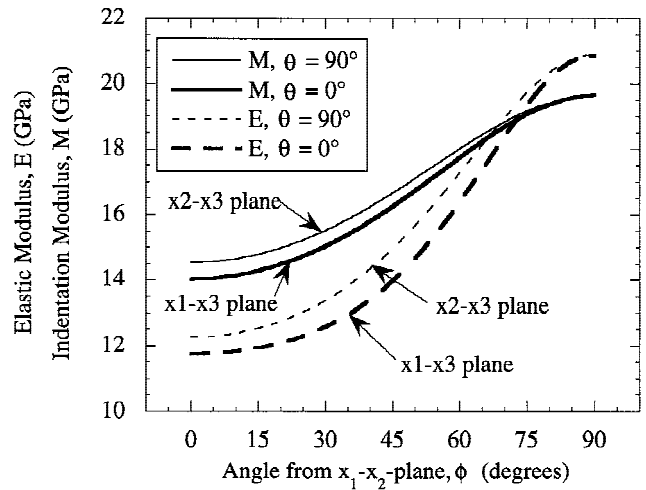


Figure 4. Elastic modulus (E) and indentation modulus (M) for conical indentation of human tibial cortical bone in the x_1 - x_3 plane and the x_2 - x_3 plane.

from the nanoindentation data are approximately 25% higher than the results determined from ultrasonic velocity measurements [$M = 19.7$ GPa and $M = 14.0$ GPa in the x_3 - and x_1 directions, respectively (Fig. 4)].

The larger modulus values found for the nanoindentation results can largely be attributed to differences in the condition of the specimens. For ultrasonic experiments the bone specimens were kept moist in a saline solution, while the specimens used for nanoindentation were dehydrated in a series of alcohol baths. Rho and Pharr²² showed in nanoindentation experiments on bovine femora that dehydration increases the indentation modulus of bone by approximately 15%. Researchers using other methods^{10,21} found that dehydration increases elastic moduli by 18–24%. After using any correction for dehydration in the range cited above (15–24%), the remaining differences between nanoindentation and ultrasonic experimental results

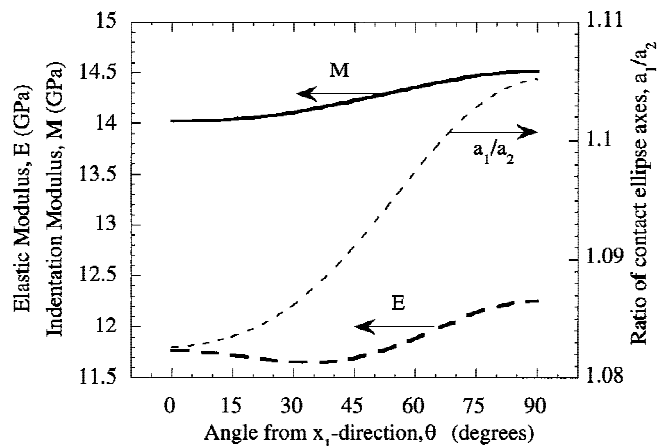


Figure 5. Elastic modulus (E), indentation modulus (M), and ratio of elliptical contact axes (a_1/a_2) for conical indentation of human tibial cortical bone in the x_1 - x_2 plane.

are not statistically significant (using a two-way analysis of variance, $p > 0.1$).

CONCLUSIONS

The results presented in this study demonstrate how the influences of elastic anisotropy are manifested in nanoindentation measurements and how nanoindentation techniques can be used to quantitatively examine bone anisotropy. This method can also be applied to other anisotropic materials. If nanoindentation data are obtained for a number of directions, the method could potentially be used to determine the anisotropic elastic constants. Although there is no inverse relationship for computing the elastic moduli directly from the indentation moduli, an iterative approach could be used.

References

1. Ascenzi A, Bonucci E. The tensile properties of single osteons. *Anat Re* 1967;158:375–386.
2. Ascenzi A, Bonucci E. The compressive properties of single osteons. *Anat Rec* 1968;161:377–392.
3. Ascenzi A, Baschieri P, Benvenuti A. The bending properties of single osteons. *J Biomech* 1990;23:763–771.
4. Ascenzi A, Baschieri P, Benvenuti A. The torsional properties of single selected osteons. *J Biomech* 1994;27:875–884.
5. Runkle JC, Pugh J. The micro-mechanics of cancellous bone. *Bull Hosp J Dis* 1975;36:2–10.
6. Townsend PR, Rose RM. Buckling studies of single human trabeculae. *J Biomech* 1975;8:199–201.
7. Ashman RB, Rho JY. Elastic moduli of trabecular bone material. *J Biomech* 1988;21:177–181.
8. Kuhn JL, Goldstein SA, Choi KW, London M, Feldkamp LA, Matthews LS. Comparison of the trabecular and cortical tissue moduli from human iliac crests. *J Orthop Res* 1989;7:876–884.
9. Mente PL, Lewis JL. Experimental method for the measurement of the elastic modulus of trabecular bone tissue. *J Orthop Res* 1989;7:456–461.
10. Ryan SD, Williams JL. Tensile testing of rod-like trabeculae excised from bovine femoral bone. *J Biomech* 1989;22:351–355.
11. Reilly DT, Burstein AH, Frankel VH. The elastic modulus of bone. *J Biomech* 1974;7:271–275.
12. Choi K, Kuhn JL, Ciarelli MJ, Goldstein SA. The elastic moduli of human subchondral trabecular and cortical bone tissue and the size-dependency of cortical bone modulus. *J Biomech* 1990;23:1103–1113.
13. Rho JY, Tsui TY, Pharr GM. Elastic properties of human cortical and trabecular bone measured by nanoindentation. *Biomater* 1997;18:1325–1330.
14. Rho JY, Roy ME II, Tsui TY, Pharr GM. Elastic properties of microstructural components of human bone tissue as measured by nanoindentation. *J Biomed Mater Res* 1999;45:48–54.
15. Zysset PK, Guo XE, Hoffler CE, Moore KE, Goldstein SA. Elastic modulus and hardness of cortical and trabecular bone lamellae measured by nanoindentation in the human femur. *J Biomech* 1999;32:1005–1012.
16. Willis JR. Hertzian contact of anisotropic bodies. *J Mech Phys Solids* 1966;14:163–176.
17. Vlassak JJ, Nix WD. Indentation modulus of elastically anisotropic half spaces. *Phil Mag A* 1993;67:1045–1056.
18. Hay JC, Sun EY, Pharr GM, Becher PF, Alexander KB. Elastic anisotropy of β -silicon nitride whiskers. *J Am Ceram Soc* 1998;81:2661–2669.
19. Swadener JG, Pharr GM. Indentation of elastically anisotropic half-spaces by cones and parabolas of revolution. *Phil Mag A*. 2001;81:447–466.
20. Rho JY. An ultrasonic method for measuring the elastic properties of human tibial cortical and cancellous bone. *Ultrasonics* 1996;34:777–783.
21. Evans FG, Lebow M. Regional differences in some physical properties of the human femur. *J Appl Physiol* 1951;3:563–572.
22. Rho JY, Pharr GM. Effects of drying on the mechanical properties of bovine femur measured by nanoindentation. *J Mater Sci Mater Med* 1999;10:485–488.
23. Pharr GM. Measurement of mechanical properties by ultra-low load indentation. *Mater Sci Eng* 1998;A253:151–159.
24. King RB. Elastic analysis of some punch problems for a layered medium. *Int J Solids Struct* 1987;23:1657–1664.
25. Larson PL, Giannakopoulos AE, Söderlund E, Rowcliffe DJ, Vestergaard R. Analysis of Berkovich indentations. *Int J Solids Struct* 1996;33:221–248.
26. Vlassak JJ, Nix WD. Measuring the elastic properties of anisotropic materials by means of indentation experiments. *J Mech Phys Solids* 1994;42:1223–1245.
27. Johnson KL. *Contact Mechanics*. Cambridge: Cambridge University Press; 1985. p 111–114.
28. Barnett DM, Lothe J. Line force loadings on anisotropic half-spaces and wedges. *Physica Norveg* 1975;8:13–22.
29. Oliver WC, Pharr GM. An improved technique for determining hardness and elastic modulus using load and displacement sensing indentation experiments. *J Mater Res* 1992;7:1564–1583.
30. Pharr GM, Oliver WC, Brotzen FR. On the generality of the relationship among contact stiffness, contact area, and elastic modulus during indentation. *J Mater Res* 1992;7:613–617.
31. Green AE, Zerna W. *Theoretical Elasticity*, 2nd ed. London: Oxford University Press; 1968. p 148–159.